

# Analysis of age-structured malaria transmission model

Joel M. Addawe<sup>1,\*</sup> , Jose Ernie C. Lope<sup>2</sup>

<sup>1</sup>Department of Mathematics and Computer Science, University of the Philippines Baguio

<sup>2</sup>Institute of Mathematics, University of the Philippines Diliman

In this paper, we propose a model to study the dynamics of malaria in an age-structured human host. Our model divides the human population into two compartments: pre-school (0-5 years) and the rest of the human population. The results of our mathematical analysis indicate that the disease-free equilibrium is asymptotically stable and occurs whenever the basic reproduction number  $R_0$  is less than unity. For  $R_0 > 1$ , the disease-free equilibrium point is unstable. Using published demographic epidemiological parameters, our numerical simulations suggest that a unique, stable endemic equilibrium exists.

## KEYWORDS

Reproduction number, malaria, transmission model, disease-free equilibrium.

## INTRODUCTION

Malaria is a vector-borne disease caused by protozoan parasites *Plasmodium falciparum* (*P. falciparum*), the species that

causes the most severe form of the disease in humans. According to the World Health Organization (WHO) Malaria Report (WHO 2008), about 3.3 billion people were at risk of malaria. Of these, around 247 million clinical episodes are reported and around one million deaths are caused by malaria every year. The majority of these deaths have been children under five (5) years. For the sub-Saharan Africa human population, malaria accounted for 18.0% (precision estimate: 15.8–20.2%) of children's death (Rowe et al. 2006).

The first malaria models were formulated by Ross (1911) and Macdonald (1957) and had major influences in later attempts to mathematically model the spread of malaria. Malaria is transmitted through the vectors, *Anopheles* mosquitos, and infects human of all ages. The disease is transmitted from person to person by female mosquito bites. Malaria infection begins with a mosquito bite that injects *P. falciparum* parasites into the human bloodstream. In a matter of minutes, the sporozoites infect the liver. In a period of two weeks, the sporozoites develop into merozoites that are then released into the blood stream where they invade red blood cells. Inside these blood cells, they grow and divide, eventually causing the rupture of the cell and the release of more merozoites. After ten days, some merozoites develop to form the release of gametocytes that are transferred to a mosquito, when a mosquito feeds on the infected human. Inside the mosquito, gametocytes mature into sporozoites and the malaria parasite cycle begins again (NIAID 2007).

There have been efforts over the last three decades to identify a vaccine against *P. falciparum* malaria. Although various control methods are beginning to result in downward trends in incidences in some countries (Breman et al. 2004), the

\*Corresponding author

Email Address: jmaddawe@up.edu.ph  
joel.addawe@gmail.com

Submitted: September 15, 2011

Revised: June 25, 2012

Accepted: July 30, 2012

Published: November 13, 2012

Editor-in-charge: Jose Ma. P. Balmaceda

gross number of malaria cases is still on the increase due to several factors including poor and ineffective diagnosis (Kiszewski and Teklehaimanot 2004). Scientists are assessing different vaccine formulations that stimulate the human immune system to control the parasite densities at particular stages of its life cycle (Beier et al. 1994, Alonso et al. 2004). Several candidate malaria vaccines are now in Phase I or Phase II clinical trials or have entered pre-clinical testing.

### Model Formulation

We analyze a model similar to that of Tumwiine et al. (2007), where the human population is divided into three compartments: susceptible humans  $S_H$ , infectious humans  $I_H$ , and recovered humans (with temporary immunity)  $R_H$ . The mosquito or vector population is divided into two compartments: the susceptible class  $S_V$  and the infectious class  $I_V$ . Our model, illustrated in Figure 1, seeks to look into the dynamics of the Susceptible-Infectious-Recovered-Susceptible and Susceptible-Infectious (SIRS-SI) malaria transmission, taking into account the two human classes, pre-school children (H1 – aged five and below) and the rest of the humans (H2 – older than five years).

The main difference of our model from that of Tumwiine et al. (2007) is that we have divided the human population into two classes: H1 and H2 having  $S$ ,  $I$  and  $R$  compartments in each class. Thus, the human population  $N_H$  is divided into six compartments denoted by the following variables:

$S_{H1}$  is the number of susceptible humans of age five (5) years and below;

$I_{H1}$  is the number of infectious humans of age five (5) years and below;

$R_{H1}$  is the number of recovered humans (with temporary immunity) of age five (5) years and below;

$S_{H2}$  is the number of susceptible humans older than five (5) years;

$I_{H2}$  is the number of infectious humans older than five (5) years; and

$R_{H2}$  is the number of recovered humans (with temporary immunity) older than five (5) years.

In general, any member of the human population (pre-school or older) remains in the susceptible class  $S$  for a certain period unless bitten and becomes infectious. Once in the infective class  $I$ , an individual may recover without acquiring immunity and be transferred back into the susceptible class  $S$ , or stays in class  $I$  while infectious before moving to the recovered class  $R$  with an acquired temporary immunity. Humans in the recovered class may lose immunity and move back to the susceptible class. Humans leave the population through natural death rate and

through per-capita death rate due to infection.

In particular, members of the susceptible pre-school humans  $S_{H1}$  leave the population and move to infectious  $I_{H1}$  or grow older to susceptible  $S_{H2}$ . Infectious  $I_{H1}$  leave the population and transfer to the infectious  $I_{H2}$ , recovered  $R_{H1}$  or back to the susceptible  $S_{H1}$ . For the recovered  $R_{H1}$  population, members may grow to the recovered  $R_{H2}$  or move to the susceptible  $S_{H1}$ .

Similarly, for the rest of the human population, susceptible  $S_{H2}$  members may move to the infectious class  $I_{H2}$ . Infectious  $I_{H2}$  members can transfer to the recovered  $R_{H2}$  or move back to susceptible  $S_{H2}$ . Recovered  $R_{H2}$  members can lose immunity and move back to the susceptible  $S_{H2}$  group.

As for the vector population  $N_V$ , it is divided into two compartments:

$S_V$  is the number of mosquitoes in the susceptible class; and

$I_V$  is the number of mosquitoes in the infectious class.

Susceptible mosquitoes  $S_V$  may transfer into the infective class  $I_V$ . Due to short life cycle of mosquitoes, the infective period ends with their death.

The movements of humans and mosquitoes from one class to another are illustrated in Figure 1 while the parameters used in the model are shown in Table 1. The human-mosquito interaction follows this system of differential equations:

$$\frac{dS_{H1}}{dt} = \lambda_H N_H - \mu_1 S_{H1} - \frac{a_1 b S_{H1} I_V}{N_H} + \gamma_1 R_{H1} + \nu_1 I_{H1} - \epsilon S_{H1}; \quad (2.1)$$

$$\frac{dS_{H2}}{dt} = -\mu_H S_{H2} - \frac{a_2 b S_{H2} I_V}{N_H} + \gamma_2 R_{H2} + \nu_2 I_{H2} + \epsilon S_{H1}; \quad (2.2)$$

$$\frac{dI_{H1}}{dt} = \frac{a_1 b S_{H1} I_V}{N_H} - \gamma_1 I_{H1} - r_1 I_{H1} - \mu_1 I_{H1} - \delta_1 I_{H1} - \epsilon I_{H1}; \quad (2.3)$$

$$\frac{dI_{H2}}{dt} = \frac{a_2 b S_{H2} I_V}{N_H} - \gamma_2 I_{H2} - r_2 I_{H2} - \mu_2 I_{H2} - \delta_2 I_{H2} + \epsilon I_{H1}; \quad (2.4)$$

$$\frac{dR_{H1}}{dt} = r_1 I_{H1} - \gamma_1 R_{H1} - \mu_1 R_{H1} - \epsilon R_{H1}; \quad (2.5)$$

$$\frac{dR_{H2}}{dt} = r_2 I_{H2} - \gamma_2 R_{H2} - \mu_2 R_{H2} + \epsilon R_{H1}; \quad (2.6)$$

$$\frac{dS_V}{dt} = \lambda_V N_V - \mu_V S_V - \frac{a_1 c S_V I_{H1}}{N_H} - \frac{a_2 c S_V I_{H2}}{N_H}; \quad (2.7)$$

$$\frac{dI_V}{dt} = \frac{a_1 c S_V I_{H1}}{N_H} + \frac{a_2 c S_V I_{H2}}{N_H} - \mu_V I_V. \quad (2.8)$$

Note that  $N_H = S_{H1} + I_{H1} + R_{H1} + S_{H2} + I_{H2} + R_{H2}$  and  $N_V = S_V$

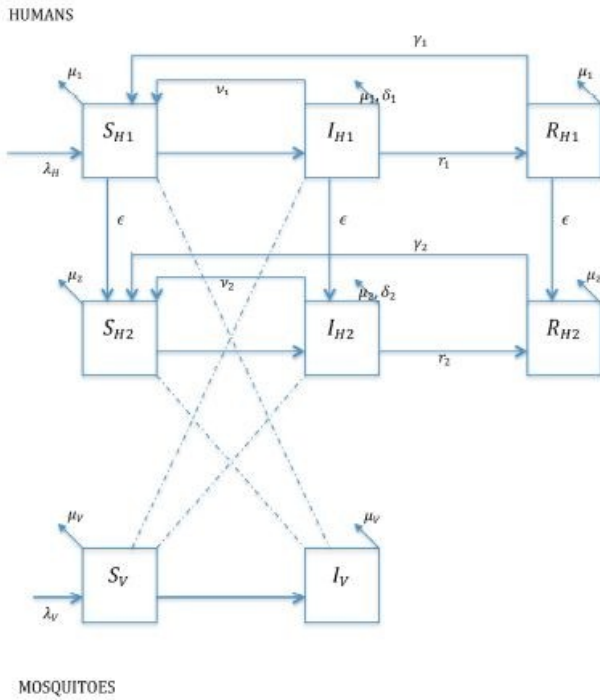


**Figure 1.** SIRS-SI with age-structured human population.

+  $I_V$ . We differentiate these equations and add the corresponding equations in (2.1) – (2.8) to obtain the differential equations:

$$\frac{dN_H}{dt} = \lambda_H N_H - \mu_1(S_{H1} + I_{H1} + R_{H1}) - \mu_2(S_{H2} + I_{H2} + R_{H2}) - \delta_1 I_{H1} - \delta_2 I_{H2};$$

$$\frac{dN_V}{dt} = (\lambda_V - \mu_V) N_V.$$

The model assumes that all newborns are susceptible in both human and mosquito populations. The per capita birth rate for humans and mosquito populations,  $\lambda_H$  and  $\lambda_V$  respectively, are both positive. The human and mosquito populations experience per capita natural death rates  $\mu_1$ ,  $\mu_2$  and  $\mu_V$ , respectively. Infected humans die due to infection at per capita death rates  $\delta_1$  and  $\delta_2$ , respectively. Recovered human individuals lose their immunity at per capita rates of  $\gamma_1$  and  $\gamma_2$ . To ensure that we have a stable positive human population, we assume that  $\lambda_H > \delta_1 + \delta_2 + \mu_1 + \mu_2$ . Moreover, it is clear that the birth rate  $\lambda_H$  should be greater than the per capita rate  $\epsilon$  of growing up.

Consider the interaction between the two populations shown in Figure 1. If  $a_1$  is the average number of bites per mosquito per unit time, then there are  $a_1 N_V / N_H$  bites per human per time. For the pre-school humans H1, note that there are  $S_{H1}$  susceptible humans and the proportion of the total number of bites that are potentially infectious to humans is  $I_V / N_V$ . Then the number of

potentially infectious bites given to susceptible pre-school humans is  $a_1 I_V S_{H1} / N_H$  bites per time. However, only a fraction of these bites, namely  $b$ , successfully infect the pre-school humans. Hence we have:

$$\frac{\text{pre-school humans infected}}{\text{unit time}} = \frac{a_1 b I_V S_{H1}}{N_H}$$

The same formulation is constructed for the rest of the human group H2:

$$\frac{\text{rest of humans infected}}{\text{unit time}} = \frac{a_2 b I_V S_{H2}}{N_H}$$

Similarly for the mosquito population, we have

$$\frac{\text{mosquitoes infected}}{\text{unit time}} = \frac{a_1 c I_{H1} S_V}{N_H} + \frac{a_2 c I_{H2} S_V}{N_H}$$

To analyze the age-structured malaria model given by Equations (2.1)–(2.8), we construct the fractional quantities by scaling the population of each class by the total species population. The proportions for the system are  $S_{h1} = S_{H1} / N_H$ ,  $I_{h1} = I_{H1} / N_H$ ,  $R_{h1} = R_{H1} / N_H$ ,  $S_{h2} = S_{H2} / N_H$ ,  $I_{h2} = I_{H2} / N_H$ ,  $R_{h2} = R_{H2} / N_H$ ,  $S_v = S_V / N_H$  and  $I_v = I_V / N_V$ . Note that we have used small letters with subscripts to denote the scaled quantities.

This creates a new system of eight equations for the fractional population variables  $S_{h1}$ ,  $I_{h1}$ ,  $R_{h1}$ ,  $S_{h2}$ ,  $I_{h2}$ ,  $R_{h2}$ ,  $S_v$  and  $I_v$  that are obtained by differentiating each proportion with respect to time. However, since we have the relations  $S_{h2} = 1 - (I_{h1} + R_{h1} + S_{h2} + I_{h2} + R_{h2})$  and  $S_v = 1 - I_v$ , we obtain the following reduced system of six differential equations:

$$\begin{aligned} \frac{dI_{h1}}{dt} &= a_1 b m (1 - (I_{h1} + R_{h1} + S_{h2} + I_{h2} + R_{h2})) I_v \\ &\quad - (v_1 + r_1 + \delta_1 + \lambda_H + \epsilon) I_{h1} \\ &\quad + (\mu_2 - \mu_1) I_{h1} (S_{h2} + I_{h2} + R_{h2}) + \delta_1 I_{h1}^2 + \delta_2 I_{h1} I_{h2}; \end{aligned} \quad (2.9a)$$

$$\begin{aligned} \frac{dR_{h1}}{dt} &= r_1 I_{h1} - R_{h1} (\gamma_1 + \epsilon + \lambda_H) + (\mu_2 \\ &\quad - \mu_1) R_{h1} (S_{h2} + I_{h2} + R_{h2}) \\ &\quad + \delta_1 I_{h1} R_{h1} + \delta_2 I_{h2} R_{h1}; \end{aligned} \quad (2.9b)$$

$$\begin{aligned} \frac{dS_{h2}}{dt} &= -(\mu_2 - \mu_1 + \lambda_H) S_{h2} + \epsilon (1 - (I_{h1} \\ &\quad + R_{h1} + S_{h2} + I_{h2} + R_{h2})) - a_2 b m S_{h2} I_v \\ &\quad + \gamma_2 R_{h2} + v_2 I_{h2} + (\mu_2 - \mu_1) S_{h2} (S_{h2} + I_{h2} \\ &\quad + R_{h2}) + \delta_1 S_{h2} I_{h1} + \delta_2 S_{h2} I_{h2}; \end{aligned} \quad (2.9c)$$

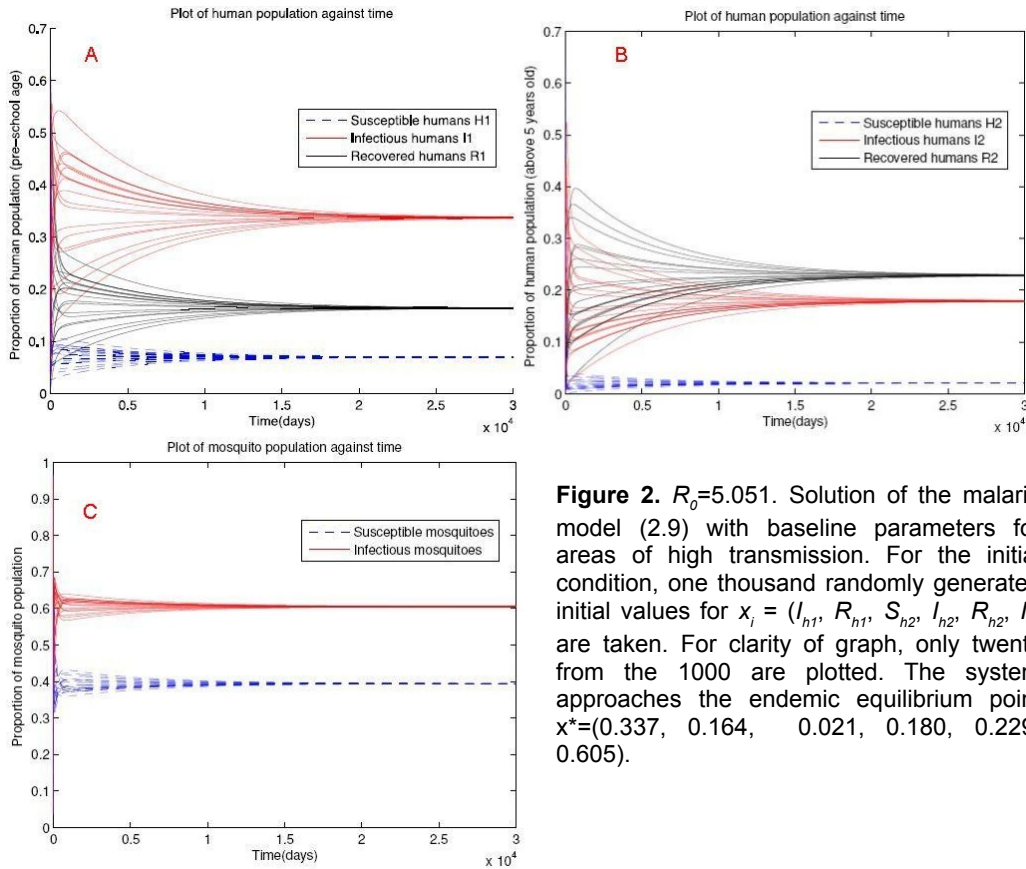


**Figure 2.**  $R_0=5.051$ . Solution of the malaria model (2.9) with baseline parameters for areas of high transmission. For the initial condition, one thousand randomly generated initial values for  $x_i = (I_{h1}, R_{h1}, S_{h2}, I_{h2}, R_{h2}, I_v)$  are taken. For clarity of graph, only twenty from the 1000 are plotted. The system approaches the endemic equilibrium point  $x^*=(0.337, 0.164, 0.021, 0.180, 0.229, 0.605)$ .

$$\frac{dI_{h2}}{dt} = a_2 b m S_{h2} I_v - (\mu_2 - \mu_1 + v_2 + r_2 + \delta_2 + \lambda_H) I_{h2} + (\mu_2 - \mu_1) I_{h2} (S_{h2} + I_{h2} + R_{h2}) + \delta_1 I_{h1} I_{h2} + \delta_2 I_{h2}^2 + \epsilon I_{h1} \quad (2.9d)$$

$$\frac{dR_{h2}}{dt} = r_2 I_{h2} - (\mu_2 - \mu_1 + \gamma_2 + \lambda_H) R_{h2} + \epsilon R_{h1} + (\mu_2 - \mu_1) R_{h2} (S_{h2} + I_{h2} + R_{h2}) + \delta_1 I_{h1} R_{h2} + \delta_2 I_{h2} R_{h2}; \quad (2.9e)$$

$$\frac{dI_v}{dt} = c(a_1 I_{h1} + a_2 I_{h2}) - (c(a_1 I_{h1} + a_2 I_{h2}) + \lambda_V) I_v. \quad (2.9f)$$

This system of equations is epidemiologically and mathematically well-posed on the domain  $D = \{(I_{h1}, R_{h1}, S_{h2}, I_{h2}, R_{h2}, I_v)^T \in \mathbb{R}_+^6 \mid I_{h1} \geq 0, R_{h1} \geq 0, S_{h2} \geq 0, I_{h2} \geq 0, R_{h2} \geq 0, 0 \leq I_{h1} + R_{h1} + S_{h2} + I_{h2} + R_{h2} \leq 1, \text{ and } 0 \leq I_v \leq 1\}$ , where  $\mathbb{R}_+^6$  denotes the positive orthant in  $\mathbb{R}^6$ .

### Model Analysis

In this section, the age-structured malaria model is

qualitatively analyzed to investigate the existence and stability of the disease-free equilibrium point. We use the reproductive ratio  $R_0$  to determine the stability of the disease-free equilibrium point. Due to the complexity arising from the six nonlinear equations, we resort to numerical simulations to assert that an endemic equilibrium point exists.

**Definition 1.** If  $f$  is a map of a set  $Y$  into itself, a subset  $X$  of  $Y$  is forward invariant under  $f$  if  $f(X) \subset X$

**Theorem 2.** Assuming that the initial conditions lie in  $D$ , the system (2.9) has a unique solution that exists and remains in  $D$  for all time  $t \geq 0$ .

**Proof:** Note that the right-hand side of the system of equations (2.9) is continuous with continuous partial derivatives in  $D$ , so (2.9) has a unique solution. To show that  $D$  is forward invariant, we note that if  $I_{h1}=0$  then  $I'_{h1} \geq 0$ ; if  $R_{h1}=0$  then  $R'_{h1} \geq 0$ ; if  $S_{h2}=0$  then  $S'_{h2} \geq 0$ ; if  $I_{h2}=0$  then  $I'_{h2} \geq 0$ ; if  $R_{h2}=0$  then  $R'_{h2} \geq 0$ ; and if  $I_v=0$  then  $I'_v \geq 0$ . Note also that if  $I_{h1} + R_{h1} + S_{h2} + I_{h2} + R_{h2}=1$  then  $I'_{h1} + R'_{h1} + S'_{h2} + I'_{h2} + R'_{h2} < 0$ . If  $I_v=0$ , then  $I'_v \geq 0$ , and when  $I_v=1$  then  $I'_v < 0$ . Hence, none of the orbits can leave  $D$  and a unique solution exists for all time.

**Definition 3.** A disease-free equilibrium (DFE) is a steady

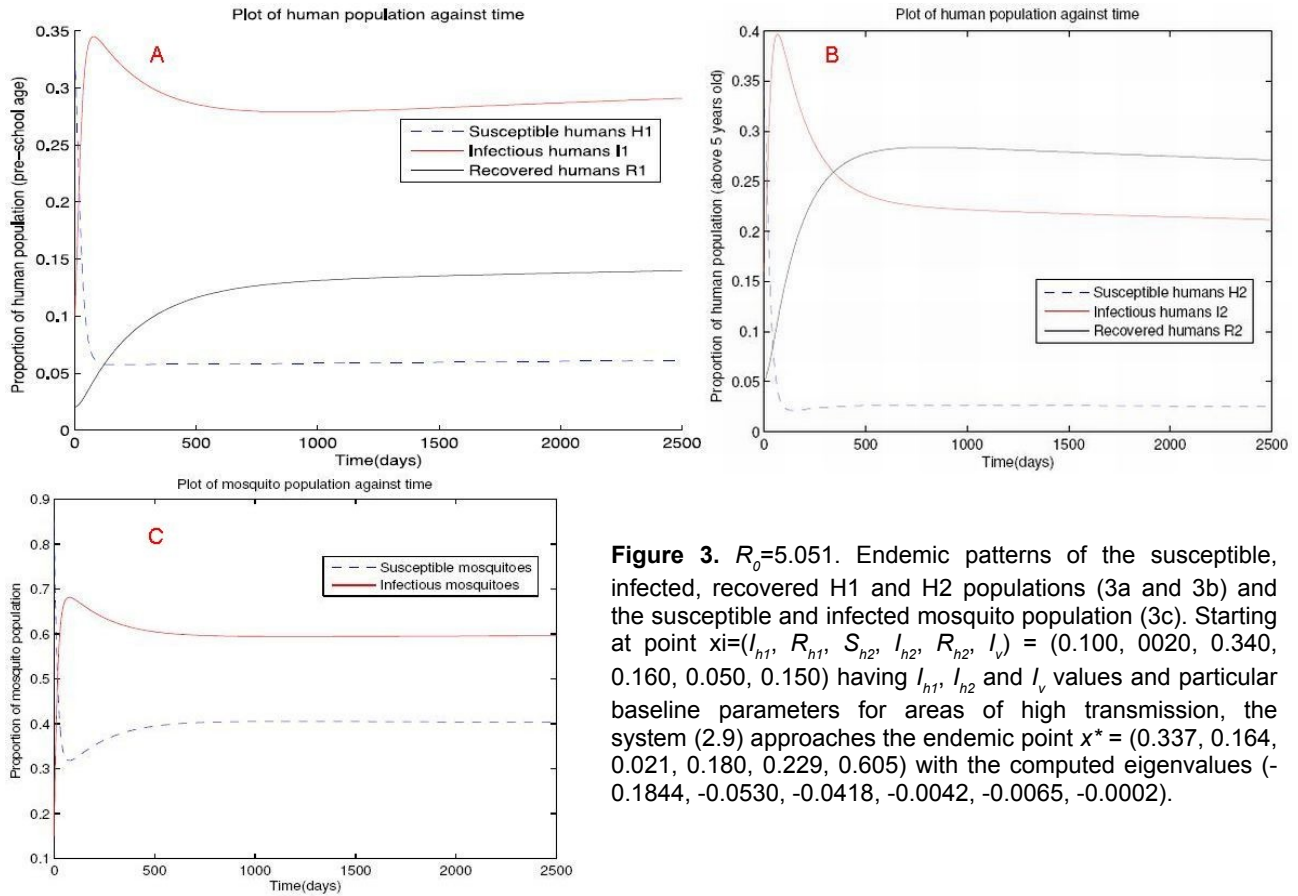


**Figure 3.**  $R_0=5.051$ . Endemic patterns of the susceptible, infected, recovered H1 and H2 populations (3a and 3b) and the susceptible and infected mosquito population (3c). Starting at point  $x_i=(I_{h1}, R_{h1}, S_{h2}, I_{h2}, R_{h2}, I_v) = (0.100, 0.020, 0.340, 0.160, 0.050, 0.150)$  having  $I_{h1}, I_{h2}$  and  $I_v$  values and particular baseline parameters for areas of high transmission, the system (2.9) approaches the endemic point  $x^* = (0.337, 0.164, 0.021, 0.180, 0.229, 0.605)$  with the computed eigenvalues  $(-0.1844, -0.0530, -0.0418, -0.0042, -0.0065, -0.0002)$ .

state solution of an epidemic model with all infected variables  $I_{h1}, I_{h2}$ , and  $I_v$  equal to zero.

**Lemma 4.** For all DFE points on

$$D \cap \partial \mathbb{R}_+^6, I_{h1} = I_{h2} = R_{h1} = R_{h2} = I_v = 0$$

**Proof:** Suppose no infected mosquitoes are present, i.e.,  $I_v=0$ . By setting the right hand side of Equation (2.9f) to zero, we see that  $I_v=0$  is true if and only if  $I_{h1}=I_{h2}=0$  is true. If  $I_{h1}=I_{h2}=0$ , and we set the right hand side of Equation (2.9b) to zero, then  $R_{h1}=0$ . Similarly, using Equation (2.9e) we get  $R_{h2}=0$ .

**Theorem 5.** The malaria model (2.9) has exactly one DFE point in  $D \cap \partial \mathbb{R}_+^6$  which we label as  $x_0 = (0,0, S_{h2}^*, 0,0,0)$  where  $S_{h2}^* = \frac{\epsilon}{\lambda_H + \epsilon}$  if  $\mu_2 - \mu_1 = 0$ , and

$$S_{h2}^* = \frac{(\mu_2 - \mu_1 + \lambda_H + \epsilon) - \sqrt{(\mu_2 - \mu_1 + \lambda_H + \epsilon)^2 - 4(\mu_2 - \mu_1)\epsilon}}{2(\mu_2 - \mu_1)} \quad \text{if } \mu_2 - \mu_1 \neq 0.$$

**Proof:** We need to show that  $x_0$  is an equilibrium point of (2.9) and no other equilibrium points exist on  $D \cap \partial \mathbb{R}_+^6$ . We can see from Lemma 4 that on  $D \cap \partial \mathbb{R}_+^6, I_{h1}^* = I_{h2}^* = R_{h1}^* = R_{h2}^* = I_v^* = 0$ . If  $S_{h2}^* = 0$ , we then get the equation  $(\mu_2 - \mu_1)(S_{h2}^*)^2 - (\mu_2 - \mu_1 + \lambda_H + \epsilon)S_{h2}^* + \epsilon = 0$ . If  $\mu_2 - \mu_1 = 0$ , then  $S_{h2}^* = \epsilon/(\lambda_H + \epsilon)$  is unique in  $D$ . If  $\mu_2 - \mu_1 \neq 0$ , we show that the only possible value is

$$S_{h2}^* = \frac{(\mu_2 - \mu_1 + \lambda_H + \epsilon) - \sqrt{(\mu_2 - \mu_1 + \lambda_H + \epsilon)^2 - 4(\mu_2 - \mu_1)\epsilon}}{2(\mu_2 - \mu_1)}. \quad (3.1)$$

We first show that

$$S_{h2}^{**} = \frac{(\mu_2 - \mu_1 + \lambda_H + \epsilon) + \sqrt{(\mu_2 - \mu_1 + \lambda_H + \epsilon)^2 - 4(\mu_2 - \mu_1)\epsilon}}{2(\mu_2 - \mu_1)}$$

is not in  $D$ . Assume that  $\mu_2 > \mu_1$ . Since  $\lambda_H > \mu_2 + \mu_1$  and  $\lambda_H > \epsilon$ ,

$$-(\mu_2 - \mu_1) + \lambda_H + \epsilon + \sqrt{(\mu_2 - \mu_1 + \lambda_H + \epsilon)^2 - 4(\mu_2 - \mu_1)\epsilon} > 0,$$

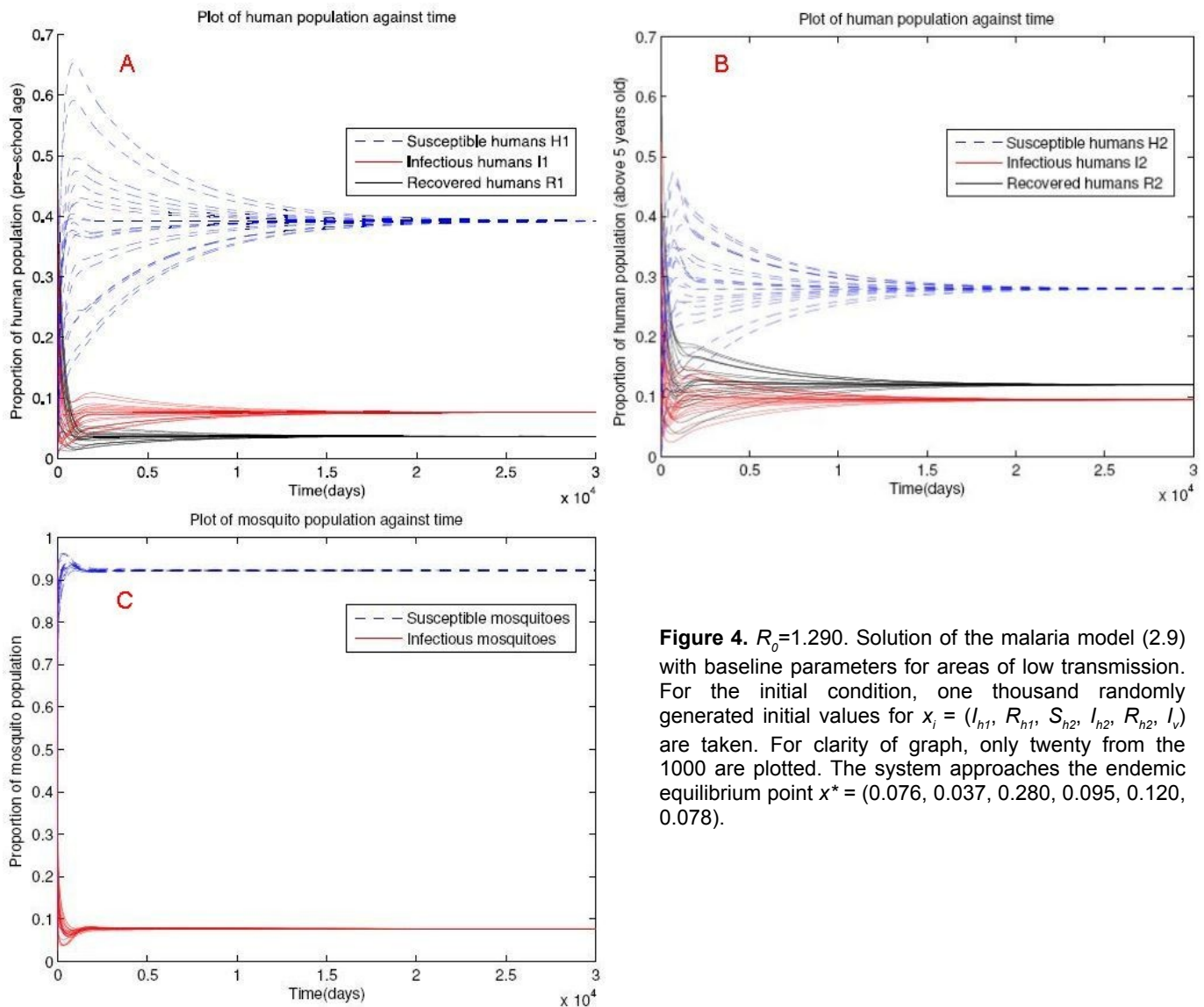


**Figure 4.**  $R_0=1.290$ . Solution of the malaria model (2.9) with baseline parameters for areas of low transmission. For the initial condition, one thousand randomly generated initial values for  $x_i = (I_{h1}, R_{h1}, S_{h2}, I_{h2}, R_{h2}, I_v)$  are taken. For clarity of graph, only twenty from the 1000 are plotted. The system approaches the endemic equilibrium point  $x^* = (0.076, 0.037, 0.280, 0.095, 0.120, 0.078)$ .

$$(\mu_2 - \mu_1 + \lambda_H + \epsilon) + \sqrt{(\mu_2 - \mu_1 + \lambda_H + \epsilon)^2 - 4(\mu_2 - \mu_1)\epsilon} > 2(\mu_2 - \mu_1),$$

which implies that  $S_{h2}^{**} > 1$  and hence, it is not in  $D$ . On the other hand, if  $\mu_2 < \mu_1$ , then by a similar reasoning, we can show that  $S_{h2}^{**} < 0$  and hence not in  $D$ .

Next, we show that  $0 < S_{h2}^* < 1$ . We again assume that  $\mu_2 > \mu_1$ , and start with the inequality  $4\lambda_H(\mu_2 - \mu_1) > 0$ . We then add the expression  $(\lambda_H + \epsilon)^2 - 2(\mu_2 - \mu_1)\epsilon - 2\lambda_H(\mu_2 - \mu_1) + (\mu_2 - \mu_1)^2$  to both sides of the inequality to get  $[(\mu_2 - \mu_1 + \lambda_H + \epsilon)^2 - 4(\mu_2 - \mu_1)\epsilon] > [\lambda_H + \epsilon - (\mu_2 - \mu_1)]^2$ . Next, we take the square root of both sides and add  $2(\mu_2 - \mu_1)$  to get

$$2(\mu_2 - \mu_1) + \sqrt{(\mu_2 - \mu_1 + \lambda_H + \epsilon)^2 - 4(\mu_2 - \mu_1)\epsilon} > (\mu_2 - \mu_1) + \lambda_H + \epsilon$$

Hence  $S_{h2}^* < 1$ . Starting with the inequality  $(\mu_2 - \mu_1 + \lambda_H + \epsilon) > \sqrt{(\mu_2 - \mu_1 + \lambda_H + \epsilon)^2 - 4(\mu_2 - \mu_1)\epsilon}$ , we can similarly arrive at  $S_{h2}^* > 0$ . Hence  $0 < S_{h2}^* < 1$ .

As for the case when  $\mu_2 < \mu_1$ , we can argue similarly to show that  $0 < S_{h2}^* < 1$  so we may omit the details.

This completes the proof that  $S_{h2}^*$  is unique in  $D$ .

### Reproductive number

**Definition 6.** The reproductive ratio  $R_0$  is the expected number of individuals infected by a single infected individual over the duration of the infectious period in a population, which is entirely susceptible.

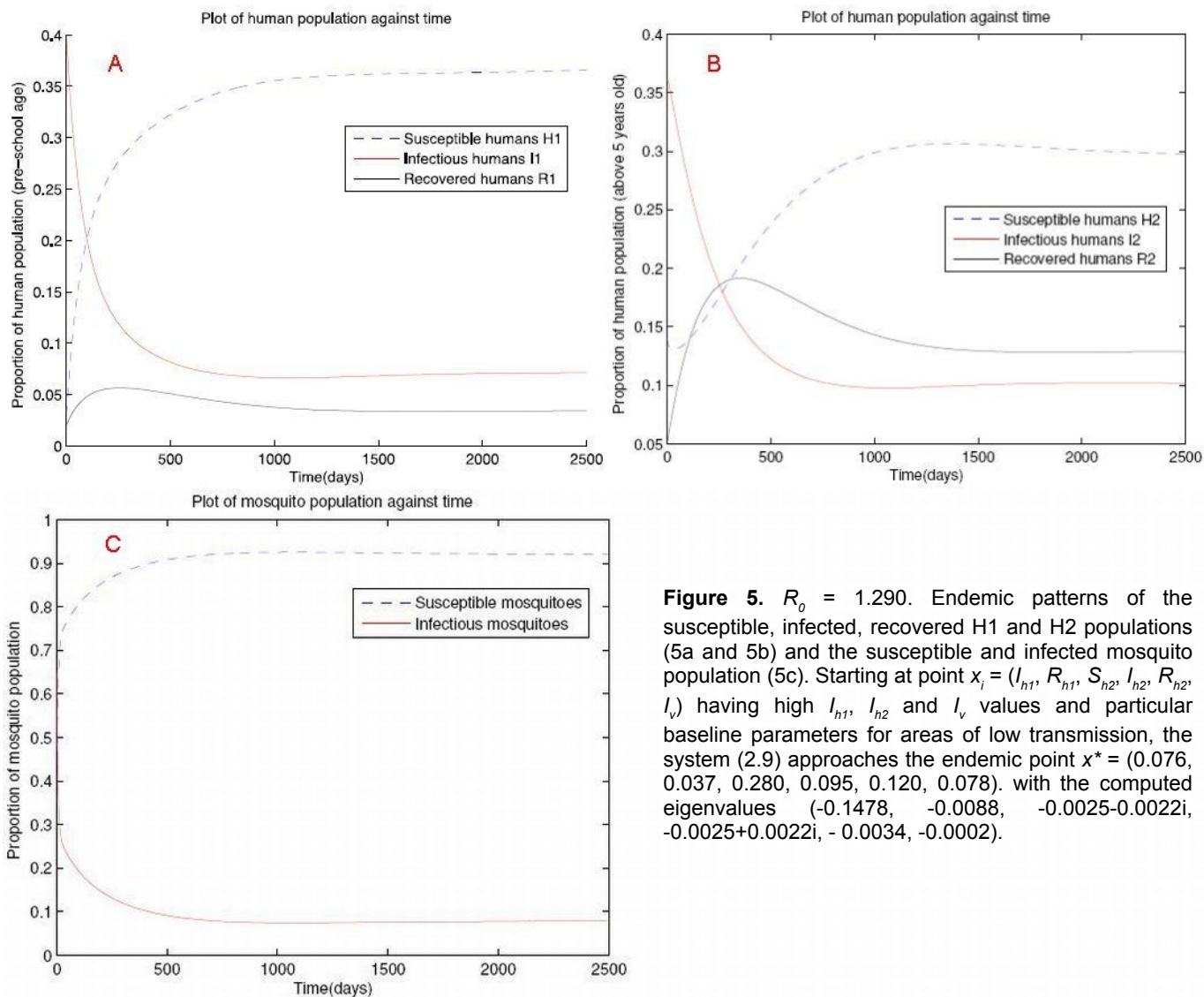


**Figure 5.**  $R_0 = 1.290$ . Endemic patterns of the susceptible, infected, recovered H1 and H2 populations (5a and 5b) and the susceptible and infected mosquito population (5c). Starting at point  $x_i = (I_{h1}, R_{h1}, S_{h2}, I_{h2}, R_{h2}, I_v)$  having high  $I_{h1}$ ,  $I_{h2}$  and  $I_v$  values and particular baseline parameters for areas of low transmission, the system (2.9) approaches the endemic point  $x^* = (0.076, 0.037, 0.280, 0.095, 0.120, 0.078)$ . with the computed eigenvalues  $(-0.1478, -0.0088, -0.0025-0.0022i, -0.0025+0.0022i, -0.0034, -0.0002)$ .

We use the next generation operator approach defined by Diekmann et al. (1990) and Van den Driessche and Watmough (2002) to compute  $R_0$ . In the next generation method,  $R_0$  is defined as the spectral radius of the next generation operator  $K$ . The formation of the operator  $K$  involves in formulating the infected and non-infected compartments from the model equation (2.9). To find the next generation operator in matrix notation, let us assume that there are  $n$  compartments of which  $m$  are infected. Define the vector  $x = x_i$  ( $i = 1, 2, \dots, n$ ), where  $x_i$  denotes the proportions in the  $i$ th compartment, and where  $x_0^* = (0, 0, S_{h2}^*, 0, 0, 0)$  is the disease-free equilibrium point. Let  $F_i(x)$  be the rate of appearance of new infections, while  $V_i(x) = V_i^-(x) - V_i^+(x)$  are the transfer of individuals out of the compartment  $i$ . We form the next generation operator  $K = FV^{-1}$  where  $F = [\partial F_i(x_0)/\partial x_j]$  and  $V = [\partial V_i(x_0)/\partial x_j]$ . Since we are concerned with the

population that spread the infection, then we only need to model  $I_{h1}$ ,  $I_{h2}$  and  $I_v$  classes. In equation (2.9), we form the equations from  $I_{h1}$ ,  $I_{h2}$  and  $I_v$  which are the expressions that refer to infections. In our model, the subscripts  $i$  and  $j$  are elements of the set  $\{1, 2, 3\}$ . Note that  $F_i$  includes only infections that are newly arising, and does not include terms that describe the transfer of infectious individuals from one infected compartment to another. Hence we have

$$F_1 = a_1 b m (1 - I_{h1} - R_{h1} - S_{h2} - I_{h2} - R_{h2}) I_v$$

$$F_2 = a_2 b m S_{h2} I_v$$

$$F_3 = c (a_1 I_{h1} + a_2 I_{h2}) (1 - I_v)$$

and

$$V_1 = (v_1 + r_1 + \delta_1 + \delta_H + \epsilon)I_{h1} - (\mu_2 - \mu_1)I_{h1}(S_{h2} + I_{h2} + R_{h2}) - \delta_1 I_{h1}^2 - \delta_2 I_{h1} I_{h2}$$

$$V_2 = (v_2 + r_2 + \delta_2 + \lambda_H + \mu_2 - \mu_1)I_{h2} - (\mu_2 - \mu_1)I_{h2}(S_{h2} + I_{h2} + R_{h2}) - \delta_1 I_{h1} I_{h2} - \delta_2 I_{h2}^2 - \epsilon I_{h1}$$

$$V_3 = \lambda_V I_V.$$

**Table 1.** The parameters for the malaria model and their dimensions.

$a_1$	: Number of bites on H1 per female mosquito per unit time, Dimension: 1/time
$a_2$	: Number of bites on H2 per female mosquito per unit time, Dimension: 1/time
$b$	: Fraction of bites that successfully infect humans Dimensionless
$c$	: Fraction of bites that successfully infect mosquitoes Dimensionless
$\lambda_H$	: Per capita birth rate of humans, Dimension: 1/time
$\lambda_V$	: Per capita birth rate of mosquitoes Dimension: 1/time
$r_1$	: Per capita rate of acquiring temporary immunity for H1 Dimension: 1/time; $1/r_1$ is the average duration of the infectious period
$r_2$	: Per capita rate of acquiring temporary immunity for H2 Dimension: 1/time; $1/r_2$ is the average duration of the infectious period
$\gamma_1$	: Per capita loss of immunity in H1, or the progression from R state to S state Dimension: 1/time; $1/\gamma_1$ is the average duration of the human temp. immunity
$\gamma_2$	: Per capita loss of immunity in H2, or the progression from R state to S state Dimension: 1/time; $1/\gamma_2$ is the average duration of the human temp. immunity
$\delta_1$	: Per capita death rate of H1 due to infection Dimension: 1/time
$\gamma_2$	: Per capita loss of immunity in H2, or the progression from R state to S state Dimension: 1/time; $1/\gamma_2$ is the average duration of the human temp. immunity
$\delta_1$	: Per capita death rate of H1 due to infection Dimension: 1/time
$\delta_2$	: Per capita death rate of H2 due to infection Dimension: 1/time
$v_1$	: Per capita rate of recovery for H1, or the progression from $I_{h1}$ to $S_{h1}$ state. Dimension: 1/time; $1/v_1$ is the average duration of H1 infectious period.
$v_2$	: Per capita rate of recovery for H1, or progression from $I_{h2}$ to $S_{h2}$ state. Dimension: 1/time; $1/v_2$ is the average duration of H2 infectious period.
$\mu_1$	: Death rate for H1 Dimension: 1/time
$\mu_2$	: Death rate for H2 Dimension: 1/time
$\mu_V$	: Death rate for mosquitoes Dimension: 1/time
$\epsilon$	: Rate of progression from H1 to H2 Dimension: humans/time
$m$	: Female vector-host ratio; $N_V/N_H$ Dimension: mosquitoes/humans

The matrices  $F$  and  $V$  are given by:

$$F = \begin{bmatrix} 0 & 0 & a_1bm(1 - S_{h2}^*) \\ 0 & 0 & a_2bmS_{h2}^* \\ ca_1 & ca_2 & 0 \end{bmatrix}$$

$$V = \begin{bmatrix} T_1 & 0 & 0 \\ -\epsilon & T_2 & 0 \\ 0 & 0 & \lambda_V \end{bmatrix},$$

where for convenience we introduce the variables

and

**Table 2.** Baseline values and ranges for the parameters for the malaria model (2.9). The parameter descriptions are given in Table 1 and explanation of the values are found in Appendix A.

	Dimension	Baseline high	Baseline low	Range
$a_1$	1/days	0.46	0.29	0.13 – 0.47
$a_2$	1/days	0.40	0.25	0.13 – 0.47
$b$	1	0.086	0.086	0.01 – 0.27
$c$	1	0.48	0.24	0.072 – 0.64
$\lambda_H$	1/days	$1.04 \times 10^{-4}$	$1.01 \times 10^{-4}$	$7.4 \times 10^{-5} - 1.2 \times 10^{-4}$
$\lambda_V$	1/days	0.071	0.071	0.02 – 0.27
$r_1$	1/days	0.0014	0.0014	0.0014 – 0.011
$r_2$	1/days	0.0035	0.0035	0.0014 – 0.011
$\gamma_1$	1/days	0.0027	0.0027	$0.011 - 5.5 \times 10^{-5}$
$\gamma_2$	1/days	0.0027	0.0027	$0.011 - 5.5 \times 10^{-5}$
$\delta_1$	1/days	$2.14 \times 10^{-6}$	$4.52 \times 10^{-7}$	$7.1 \times 10^{-10} - 2.3 \times 10^{-6}$
$\delta_2$	1/days	$9.78 \times 10^{-8}$	$1.74 \times 10^{-7}$	$1.5 \times 10^{-8} - 5.0 \times 10^{-7}$
$v_1$	1/days	0.0083	0.0083	0.0014 – 0.011
$v_2$	1/days	0.0014	0.0014	0.0014 – 0.011
$\mu_1$	1/days	$3.27 \times 10^{-5}$	$1.99 \times 10^{-6}$	$4.6 \times 10^{-8} - 3.3 \times 10^{-5}$
$\mu_2$	1/days	$1.23 \times 10^{-5}$	$9.82 \times 10^{-7}$	$2.6 \times 10^{-8} - 1.23 \times 10^{-5}$
$\mu_V$	1/days	0.052	0.052	$1.0 \times 10^{-6} - 0.001$
$\epsilon$	Humans/days	$6.92 \times 10^{-5}$	$9.86 \times 10^{-5}$	$3.8 \times 10^{-5} - 1.2 \times 10^{-4}$
$m$	Mosquito/humans	2.0	1.0	0.001 –

$$T_1 = v_1 + r_1 + \delta_1 + \lambda_H + \epsilon - (\mu_2 - \mu_1)S_{h2}^*, \quad (3.2)$$

$$T_2 = v_2 + r_2 + \delta_2 + \lambda_H + (\mu_2 - \mu_1)(1 - S_{h2}^*). \quad (3.3)$$

Hence we have the next generation matrix

$$K = FV^{-1} = \begin{bmatrix} 0 & 0 & \frac{a_1bm(1 - S_{h2}^*)}{\lambda_V} \\ 0 & 0 & \frac{a_2bmS_{h2}^*}{\lambda_V} \\ \frac{ca_1}{T_1} + \frac{ca_2\epsilon}{T_1T_2} & \frac{ca_2}{T_2} & 0 \end{bmatrix}.$$

Taking the dominant eigenvalue of matrix  $K$ , we get

$$R_0 = \sqrt{\frac{a_1bm(1 - S_{h2}^*)}{\lambda_V} \left( \frac{ca_1}{T_1} + \frac{ca_2\epsilon}{T_1T_2} \right) + \frac{a_2^2bcmS_{h2}^*}{\lambda_V T_2}} \quad (3.4)$$

or

$$R_0^2 = \frac{a_1bm(1 - S_{h2}^*)}{\lambda_V} \left( \frac{ca_1}{T_1} + \frac{ca_2\epsilon}{T_1T_2} \right) + \frac{a_2^2bcmS_{h2}^*}{\lambda_V T_2} \quad (3.5)$$

### Stability of the disease-free equilibrium point

The stability of the equilibrium point can be performed by calculating the roots of the eigen-equation

$$\det(J^* - I\eta) = 0, \quad (3.6)$$

where  $J^*$  is the Jacobian evaluated at the equilibrium point, and  $I$  is the identity matrix. The characteristic polynomial is of degree 6 since there are six differential equations. If all the eigenvalues have negative real part, then the equilibrium point is stable.

We study the stability of the disease free equilibrium point  $x_0 = (0, 0, S_{h2}^*, 0, 0, 0)$ . The Jacobian of the malaria model (2.9) is given by:

$$J = \begin{bmatrix} J_{11} & J_{12} & J_{13} & J_{14} & J_{15} & J_{16} \\ J_{21} & J_{22} & J_{23} & J_{24} & J_{25} & 0 \\ J_{31} & J_{32} & J_{33} & J_{34} & J_{35} & J_{36} \\ J_{41} & 0 & J_{43} & J_{44} & J_{45} & J_{46} \\ J_{51} & J_{52} & J_{53} & J_{54} & J_{55} & 0 \\ J_{61} & 0 & 0 & J_{64} & 0 & J_{66} \end{bmatrix}$$

where

$$J_{11} = -a_1bml_v - (v_1 + r_1 + \delta_1 + \lambda_H + \epsilon) + (\mu_2 - \mu_1)(S_{h2} + I_{h2} + R_{h2}) + 2\delta_1I_{h1} + \delta_2I_{h2}$$

$$J_{12} = -a_1bml_v$$

$$J_{13} = -a_1bml_v + (\mu_2 - \mu_1)I_{h1}$$

$$J_{14} = -a_1bml_v + (\mu_2 - \mu_1)I_{h1} + \delta_2I_{h1}$$

$$J_{15} = -a_1bml_v + (\mu_2 - \mu_1)I_{h1}$$

$$J_{16} = a_1bm(1 - (I_{h1} + R_{h1} + S_{h2} + I_{h2} + R_{h2}))$$

$$J_{21} = r_1 + \delta_1R_{h1}$$

$$J_{22} = -(\gamma_1 + \epsilon + \lambda_H) + (\mu_2 - \mu_1)(S_{h2} + I_{h2} + R_{h2}) + \delta_1I_{h1} + \delta_2I_{h2}$$

$$J_{23} = (\mu_2 - \mu_1)R_{h1}$$

$$J_{24} = (\mu_2 - \mu_1)R_{h1} + \delta_2R_{h1}$$

$$J_{25} = (\mu_2 - \mu_1)R_{h1}$$

$$J_{31} = -\epsilon + \delta_1S_{h2}$$

$$J_{32} = -\epsilon$$

$$J_{33} = -(\mu_2 - \mu_1 + \lambda_H) - \epsilon - a_2bml_v + (\mu_2 - \mu_1)(S_{h2} + I_{h2} + R_{h2}) + (\mu_2 - \mu_1)S_{h2}$$

$$J_{34} = -\epsilon + v_2 + (\mu_2 - \mu_1)S_{h2} + \delta_2S_{h2}$$

$$J_{35} = -\epsilon + \gamma_2 + (\mu_2 - \mu_1)S_{h2}$$

$$J_{36} = -a_2bmS_{h2}$$

$$J_{41} = \delta_1I_{h2} + \epsilon$$

$$J_{43} = a_2bml_v + (\mu_2 - \mu_1)I_{h2}$$

$$J_{44} = -(\mu_2 - \mu_1 + v_2 + r_2 + \delta_2 + \lambda_H) + (\mu_2 - \mu_1)(S_{h2} + I_{h2} + R_{h2}) + (\mu_2 - \mu_1)I_{h2} + \delta_1I_{h1} + 2\delta_2I_{h2}$$

$$J_{45} = (\mu_2 - \mu_1)I_{h2}$$

$$J_{46} = a_2bmS_{h2}$$

$$J_{51} = \delta_1R_{h2}$$

$$J_{52} = \epsilon$$

$$J_{53} = (\mu_2 - \mu_1)R_{h2}$$

$$J_{54} = r_2 + (\mu_2 - \mu_1)R_{h2} + \delta_2R_{h2}$$

$$J_{55} = -(\mu_2 - \mu_1 + \gamma_2 + \lambda_H) + (\mu_2 - \mu_1)(S_{h2} + I_{h2} + R_{h2}) + (\mu_2 - \mu_1)R_{h2} + \delta_1I_{h1} + \delta_2I_{h2}$$

$$J_{61} = a_1c - a_1cI_v$$

$$J_{64} = a_2c - a_2cI_v$$

$$J_{66} = -(c(a_1I_{h1} + a_2I_{h2}) + \lambda_v)$$

**Theorem 7.** The disease free equilibrium point  $x_0$  is locally asymptotically stable if the  $R_0 < 1$  and unstable if  $R_0 > 1$ .

**Proof:** Let the eigenvalues be  $\eta_1, \eta_2, \dots, \eta_6$ . Evaluating the Jacobian matrix  $x_0$  gives us:

$$J(x_0) = \begin{bmatrix} J_{11}(x_0) & 0 & 0 & 0 & 0 & J_{16}(x_0) \\ 0 & J_{22}(x_0) & 0 & 0 & 0 & 0 \\ J_{31}(x_0) & J_{32}(x_0) & J_{33}(x_0) & J_{34}(x_0) & J_{35}(x_0) & J_{36}(x_0) \\ J_{41}(x_0) & 0 & 0 & J_{44}(x_0) & 0 & J_{46}(x_0) \\ 0 & J_{52}(x_0) & 0 & J_{54}(x_0) & J_{55}(x_0) & 0 \\ J_{61}(x_0) & 0 & 0 & J_{64}(x_0) & 0 & J_{66}(x_0) \end{bmatrix}$$

As the third column contains only the diagonal term, then this diagonal term forms one eigenvalue of the Jacobian:

$$\begin{aligned} \eta_1 &= -(\mu_2 - \mu_1 + \lambda_H) - \epsilon + 2(\mu_2 - \mu_1)S_{h2}^* \\ &= -\sqrt{(\mu_2 - \mu_1 + \lambda_H + \epsilon)^2 - 4(\mu_2 - \mu_1)\epsilon} \end{aligned}$$

Similarly, the other eigenvalues are:

$$\begin{aligned} \eta_2 &= -(\mu_2 - \mu_1 + \gamma_1 + \lambda_H) + (\mu_2 - \mu_1)S_{h2}^* \\ \eta_3 &= -(\gamma_1 + \epsilon + \lambda_H) + (\mu_2 - \mu_1)S_{h2}^* \end{aligned}$$

Note that the eigenvalues  $\eta_1, \eta_2$  and  $\eta_3$  are all negative.

The remaining eigenvalues can be obtained by solving the equation  $\eta^3 + A_1\eta^2 + A_2\eta + A_3 = 0$ , where  $A_1, A_2$ , and  $A_3$  are the coefficients given by the expressions:

$$\begin{aligned} A_1 &= -(J_{11}(x_0) + J_{44}(x_0) + J_{66}(x_0)) \\ A_2 &= -(J_{61}(x_0)J_{16}(x_0) + J_{46}(x_0)J_{64}(x_0) \\ &\quad - J_{11}(x_0)J_{44}(x_0) - J_{66}(x_0)(J_{11}(x_0) + J_{44}(x_0))) \\ A_3 &= -(-J_{46}(x_0)J_{64}(x_0)J_{11}(x_0) - J_{61}(x_0)J_{16}(x_0)J_{44}(x_0) \\ &\quad + J_{11}(x_0)J_{44}(x_0)J_{66}(x_0) + J_{16}(x_0)J_{41}(x_0)J_{64}(x_0)) \end{aligned}$$

Using Routh-Hurwitz criteria (Edelstein-Keshet 1988), the equilibrium is locally stable if the following conditions are satisfied:

- (i)  $A_1 > 0$ ;
- (ii)  $A_3 > 0$ ;

$$(iii) A_2A_1 > A_3.$$

To show (i), (ii), and (iii) we use (3.2) and (3.3). We have

$$\begin{aligned} A_1 &= (v_1 + r_1 + \delta_1 + \lambda_H + \epsilon) - (\mu_2 - \mu_1)S_{h2}^* \\ &\quad + (\mu_2 - \mu_1 + v_2 + r_2 + \delta_2 + \lambda_H) \\ &\quad - (\mu_2 - \mu_1)S_{h2}^* + \lambda_v \\ &= T_1 + T_2 + \lambda_v. \end{aligned}$$

Clearly,  $A_1 > 0$ . As for  $A_3$ , we have

$$\begin{aligned} A_3 &= -(a_2^2bcmS_{h2}^*T_1) - (a_1^2bcmT_2)(1 - S_{h2}^*) \\ &\quad + T_1T_2\lambda_v - a_1a_2bcm(1 - S_{h2}^*)\epsilon \end{aligned}$$

Recall that  $0 < S_{h1} < 1$ , so for ease of notation we introduce the positive expressions,

$$T_3 = a_1^2bcm(1 - S_{h2}^*) \tag{3.8}$$

and

$$T_4 = a_2^2bcm S_{h2}^* \tag{3.9}$$

Hence we get

$$\begin{aligned} A_3 &= T_1T_2\lambda_v - T_2T_3 - T_1T_4 \\ &\quad - \epsilon a_1a_2bcm(1 - S_{h2}^*). \end{aligned} \tag{3.10}$$

If  $R_0^2 < 1$  in (3.5), then

$$\frac{a_1bm(1 - S_{h2}^*)}{\lambda_v} \left( \frac{ca_1}{T_1} + \frac{ca_2\epsilon}{T_1T_2} \right) + \frac{a_2^2bcmS_{h2}^*}{\lambda_vT_2} < 1$$

which implies that

$$T_1T_2\lambda_v - T_2T_3 - T_1T_4 > \epsilon a_1a_2bcm(1 - S_{h2}^*).$$

Hence we have  $A_3 > 0$ .

Finally, we show that  $A_2A_1 - A_3 > 0$ . The expression for  $A_2$  is

$$\begin{aligned} A_2 &= -(a_1^2bcm)(1 - S_{h2}^*) - (a_2^2bcm S_{h2}^*) \\ &\quad + [-(v_1 + r_1 + \delta_1 + \lambda_H + \epsilon) \\ &\quad + (\mu_2 - \mu_1)S_{h2}^*](-\mu_2 + \mu_1 - v_2 - r_2 \\ &\quad - \delta_2 - \lambda_H) + (\mu_2 - \mu_1)S_{h2}^* \\ &\quad + [-(v_1 + r_1 + \delta_1 + \lambda_H + \epsilon) + (\mu_2 - \mu_1)S_{h2}^*] \\ &\quad + (\mu_2 - \mu_1)S_{h2}^* + (-\mu_2 - \mu_1 + v_2 + r_2 \\ &\quad + \delta_2 + \lambda_H) + (\mu_2 - \mu_1)S_{h2}^*](-\lambda_v) \end{aligned}$$

$$\begin{aligned}
&= -a_1^2bcm(1 - S_{h2}^*) - a_2^2bcmS_{h2}^* + T_1T_2 \\
&\quad - (\lambda_V)(\mu_2 - \mu_1 + r_1 + r_2 + v_1 + v_2 \\
&\quad + \delta_1 + \delta_2 + 2\lambda_H + \epsilon - 2(\mu_2 - \mu_1)S_{h2}^*) \\
&= -a_1^2bcm(1 - S_{h2}^*) - a_2^2bcmS_{h2}^* \\
&\quad + T_1T_2 + \lambda_V(T_1 + T_2)
\end{aligned}$$

$$A_2 = T_1T_2 + \lambda_V(T_1 + T_2) - T_3 - T_4. \quad (3.11)$$

Hence we get

$$\begin{aligned}
A_2A_1 - A_3 &= T_1^2T_2 + T_1T_2^2 + 2T_1T_2\lambda_V \\
&\quad + (T_1^2\lambda_V + T_1\lambda_V^2) + (T_2^2\lambda_V + T_2\lambda_V^2) \\
&\quad - T_3(T_1 + \lambda_V) - T_4(T_2 + \lambda_V) \\
&\quad + \epsilon a_1a_2bcm(1 - S_{h2}^*). \quad (3.12)
\end{aligned}$$

If  $R_0^2 < 1$ , then

$$T_2T_3 + T_1T_4 + \epsilon a_1a_2bcm(a - s_{h2}^*) < T_1T_2\lambda_V. \quad (3.13)$$

Since all the  $T_i$  are positive, we can see from (3.13) that

$$T_1\lambda_V > T_3 \quad (3.14)$$

and

$$T_2\lambda_V > T_4. \quad (3.15)$$

Combining (3.12), (3.14) and (3.15), we get

$$\begin{aligned}
A_2A_1 - A_3 &> T_1^2T_2 + T_1T_2^2 + 2T_1T_2\lambda_V \\
&\quad + \epsilon a_1a_2bcm(1 - S_{h2}^*),
\end{aligned}$$

and thus,  $A_2A_1 - A_3 > 0$

So if  $R_0^2 < 1$  we have shown that all the remaining eigenvalues of the Jacobian have negative real part. Hence, the disease free equilibrium point  $x_0 = (0,0, S_{h2}^*, 0,0,0)$  is locally asymptotically stable if  $R_0 < 1$ . If  $R_0^2 > 1$ , we can see that  $A_3 < 0$ . Hence, there is only one sign change in the sequence,  $A_1, A_2, A_3$  and so by Descartes rule of sign, there is one eigenvalue with positive real part. This implies that the disease-free equilibrium point  $x_0$  is unstable. If  $R_0^2 = 1$ , we have  $A_3 = 0$ , hence the Jacobian of (2.9) has one eigenvalue

equal to zero at  $R_0 = 1$ . This result makes sense intuitively, since if  $R_0 < 1$ , on the average, each infected human infects less than other human, so we expect the disease to die out.

### Endemic disease equilibrium point

The endemic equilibrium solution of (2.9) can be found by setting the right hand side to zero and solving the nonlinear system to obtain  $x^* = (I_{h1}^*, R_{h1}^*, S_{h2}^*, I_{h2}^*, R_{h2}^*, I_v^*)$ . The equilibrium point at the endemic level has a strong influence in the behavior of the disease transmission for a given community. The endemic equilibrium point is the final reachable situation, even though there could be infinitely many different initial distributions of malaria in a community. Stability analysis is an important mathematical tool that provides the conditions that guarantee the stability of an endemic equilibrium point. However, the complexity of the system of equations (2.9) has prevented us from finding explicit expressions for the representation of the endemic equilibrium point(s). Although we cannot analytically prove the existence of an endemic equilibrium point, our exhaustive numerical simulations suggest that a unique and stable equilibrium point exists.

In our numerical simulations, we made use of two sets of baseline parameter values: one for areas of high transmission and one for low transmission. According to the WHO world malaria report (2008), areas of high transmission are countries where the reported incidence of malaria due to all species is 1 or more per 1000 population per year, and for areas of low transmission are countries with less than 1 per 1000 population per year but greater than 0. Since published data (WHO 2010) about human population with reported cases such as death and admission due to malaria are accessible, then we use these parameters in our simulation. Due to lack of consistent historical data for most of the regions, we select only countries with reported number of malaria cases for the year 2009. The demographic data for countries with areas of low transmission level are from Madagascar, Rwanda, and Swaziland. Ethiopia, Sao Tome and Principe, Senegal, and Zambia are the countries chosen for areas of high malaria transmission. For the other parameter estimates, we use parameter values from published studies and country-wide data.

For each set of parameters, we numerically explore the behavior of the system and demonstrate the existence of an endemic equilibrium point for (2.9). After an endemic equilibrium point is generated, we then evaluate the eigenvalue equation to check if there is a stable endemic equilibrium point.

### Numerical Simulation Results

We present numerical simulations to illustrate the transmission of malaria disease for the two situations described above. The `ode45` and `fsolve` functions in Matlab were used in this study. The parameter values considered in the two situations are given in Table 2. For both set of parameters, we used 1000 randomly generated initial points in  $D$  and solve (2.9).

For clarity, only twenty out of the 1000 curves are shown in the graphs.

For the baseline parameters for areas of high transmission, we obtained numerically  $R_0=5.051$ . Figures 2a, 2b and 2c show the behavior for H1, H2 and mosquito populations respectively. The graphs were obtained by varying the starting points while the other parameters were fixed. Figure 2a shows the different initial and long term behavior of the H1 populations in the following classes: Susceptible pre-school  $S_{h1}$ , Infectious pre-school  $I_{h1}$ , and Recovered pre-school  $R_{h1}$ . Similarly, Figure 2b shows the different initial and long term behavior of the H2 populations in the  $S_{h2}$ ,  $I_{h2}$  and  $R_{h2}$  classes. Figure 2c shows the different initial and long term behavior of the  $S_v$  and  $I_v$  classes. As time progresses and increases further, the population in the different classes from different initial starting points seem not to change and approach a single value. For the different initial conditions, the figures illustrate to have reached an endemic equilibrium point  $x^*$ .

To explore and demonstrate stability of the steady state, the initial conditions were chosen by giving small values for infectious  $I_{h1}$  and  $I_{h2}$  on the computed endemic point. In Figure 3a, during the first few months, the susceptible pre-school humans decrease while infectious and recovered pre-school humans increase and the infectious mosquitoes also increase. Those pre-school humans who are infectious enter the infectious H2 class or may recover with partial immunity and stays in the pre-school, which explains the increase in the infectious H2 class as seen in Figure 3b. As infectious humans H1 and H2 increase, susceptible mosquitoes decrease due to the increase of infection. After the first few years, the human and mosquito populations seem to attain a situation where there is no sudden change. As time increases further the populations in the respective classes seem not to change. This is a situation when an epidemic occurs in a community and would have reached an endemic equilibrium point.

For areas of low malaria transmission as shown in Figures 4a-4c and 5a-5c, a similar approach is done. In this case, some of the baseline parameters of the malaria model have lower values. These set of parameters give rise to  $R_0 = 1.290$  and as this is greater than one the interaction is persistent. The graphs were obtained by using the baseline low parameters given in Table 2. Figures 4a, 4b and 4c show the different initial and long term behavior of the  $S_{h1}$ ,  $I_{h1}$ ,  $R_{h1}$ ,  $S_{h2}$ ,  $I_{h2}$ ,  $R_{h2}$ ,  $S_v$  and  $I_v$  classes. The numerical simulation shows the disease establishes itself in the community when  $R_0 > 1$ . Like in the case for areas of high transmission, the population in the different classes from different initial starting points reached a single value.

## SUMMARY AND CONCLUDING REMARKS

We proposed a model for the dynamics of malaria with age-structured human hosts. We analyzed a system of differential equations model with six variables for humans and two variables for mosquitoes. We showed that there exists a domain where the

model is epidemiologically and mathematically well posed. The model was then reformulated in terms of the proportions of the age-structured classes of the respective populations. The disease-free equilibrium point was obtained and its stability was analyzed. We identified the basic reproduction number  $R_0$  in terms of the model parameters that measure the intensity of the transmission of the disease. It was shown that  $R_0$  provides the expected number of new infections (in mosquitoes and humans) from one infectious individual (human or mosquito) over the duration of the infectious period. It was also established that for the basic reproduction number  $R_0 < 1$ , the disease free equilibrium point emerges. Although we cannot prove in general that the endemic equilibrium point is unique for  $R_0 > 1$ , numerical results for the selected parameter sets seem to suggest that there is a unique endemic equilibrium point.

## FOR FURTHER EXPLORATIONS

Since we have shown an explicit expression for  $R_0$ , we can analytically evaluate its sensitivity to the different parameter values. We can also numerically evaluate the sensitivity of the endemic equilibrium to the parameter values, as this will allow us to determine the relative importance to the age-structured malaria transmission and prevalence.

## CONFLICTS OF INTERESTS

The authors certify that there is no conflict of interest arising from this study including the publication of the paper.

## CONTRIBUTION OF INDIVIDUAL AUTHORS

Joel M. Addawe. The main author and researcher in this paper. This study is part of his Ph.D dissertation.

Jose Ernie C. Lope. Guided the main author all throughout the formulation and analysis of the model.

## REFERENCES

- Alonso P, Sacarlal J, Aponte J, Leach A, Macete E, Milman J, Mandomando I, Spiessens B, Guinovart C, Espasa M. Efficacy of the rts,s/as02a vaccine against infection and disease in young African children: randomized controlled trial. *The Lancet* 2004; 364(9443):1411–1420.
- Beier JC, Oster CN, Onyango FK, Bales JD, Sherwood JA, Perkins PV, Chumo DK, Koech DV, Whitmire RE, Roberts CR. *Plasmodium falciparum* incidence relative to entomologic inoculation rates at a site proposed for testing malaria vaccines in western Kenya. *Am J Trop Med Hyg* 1994; 50:529-536.
- Bekessy A, Molineaux L, Storey J. Estimation of incidence and recovery rates of *Plasmodium falciparum* parasitemia from longitudinal data. *Bull World Health Organ* 1976, 54:686-691.
- Bloland PB, Williams HA, Roundtable on the Demography of forced migration, and Joseph L. Mailman School of Public Health. Program and forced migration and health. *Malaria*

- control during mass population movements and natural disasters, National Academies Press, Washington DC, 2002.
- Boyd MF. Epidemiology: Factors related to the definitive host. In *Malariaology*, vol. 1. M.F. Boyd, ed., W.B. Saunders, Philadelphia, 1941, 608-697.
- Breman JG, Alilio MS, Mills A. Conquering the intolerable burden of malaria: What's new, what's needed: A summary. *Am J Trop Med Hyg* 2004; 71(suppl 2):1-15.
- Central Intelligence Agency, CIA - The World Factbook: <https://www.cia.gov/library/publications/the-world-factbook/>
- Chitnis N, Hyman JM, Cushing JM. Determining the important parameters in the spread of malaria through the sensitivity analysis of a mathematical model. *Bull Math Biol* 2008; 70:1272-1296.
- Davidson G, Draper CC. Field study of some of the basic factors concerned in the transmission of malaria. *Trans Roy Soc Trop Med Hyg* 1953; 47:522-535.
- Diekmann O, Heesterbeek JAP, Metz JAJ. On the definition and the computation of the basic reproductive rati $\theta$  in models for infectious diseases in heterogeneous populations. *J Math Biol* 1990; 28:365-383.
- Draper CC. Observation on the infectiousness of gametocytes in hyperendemic malaria. *Trans Roy Soc Trop Med Hyg* 1953; 47:160-165.
- Edelstein-Keshet, L. *Mathematical Models in Biology*, New York: Random House, Inc., 1988, 231-236.
- Fontenille D, Lochouart L, Diatta M, Sokhna C, Dia I, Diagne N, Lemasson J, Ba K, Tall A, Rogier C, Trape J. Four years' entomological study of the transmission of seasonal malaria in Senegal and the bionomics of *Anopheles gambiae* and *A. arabiensis*. *Trans Roy Soc Trop Med Hyg* 1997; 91:647-652.
- Garrett-Jones C, Shidrawi GR. Malaria vectorial capacity of a population of *Anopheles gambiae*. *Bull World Health Organ* 1969; 40:531-545.
- Gemperli A, Vounatsou P, Sogoba N, Smith T. Malaria Mapping Using Transmission Models: Application to Survey Data from Mali. *Am J Epidemiol* 2007; 163:289-297.
- Kiszewski A, Teklehaimanot A. A review of the clinical and epidemiological burdens of epidemic malaria. *Am J Trop Med Hyg* 2004; 179(suppl 2):128-135.
- Khan AQ, Talibi SA. Epidemiological assessment of malaria transmission in an endemic area of East Pakistan and the significance of congenital immunity. *Bull World Health Organ* 1972; 46:783-792.
- Krafsur ES, Armstrong JC. An integrated view of entomological and parasitological observations on falciparum malaria in Gambela, Western Ethiopian Lowlands. *Trans Roy Soc Trop Med Hyg* 1978; 72:348-356.
- Macdonald G. The epidemiology and control of malaria. *Trop Dis Bull* 1957; 47:907-914.
- Molineaux L, Gramiccia G. The Garki Project, World Health Organization, Geneva, 1980.
- Molineaux L, Shidrawi GR, Clarke JL, Boulzaguet JR, Ashkar TS. Assessment of insecticidal impact on the malaria mosquito's vectorial capacity, from data on the man-biting rate and age-composition. *Bull World Health Organ* 1979; 57:265-274.
- Murhead-Thomson RC. The malarial infectivity of an African village population to mosquitoes (*Anopheles gambiae*): A random xenodiagnostic survey. *Am J Trop Med Hyg* 1957; 6:971-979.
- National Institute of Allergy and Infectious Diseases (NIAID). *Understanding Malaria: Fighting an ancient scourge*. 2007. (NIH Publication No. 07-7139).
- Nedelman J. Inoculation and recovery rates in the malaria model of Dietz, Molineaux and Thomas. *Math Biosci* 1984; 69:209-233.
- Nedelman J. Introductory Review: Some new thoughts about some old malaria models. *Math Biosci* 1985; 73:159-182.
- Olayemi IK, Ande AT. Life table analysis of *Anopheles gambiae* (Diptera:Culicidae) in relation to malaria transmission. *J Vector Borne Dis* 2009; 46:295-298.
- Peters W, Standfast HA. Studies on the epidemiology of malaria in New Guinea. II. Holoendemic malaria the entomological picture. *Trans Roy Soc Trop Med Hyg* 1960; 54:249-260.
- Pull JH, Grab B. A simple epidemiological model for evaluating the malaria inoculation rate and the risk of infection in infants. *Bull World Health Organ* 1974; 51:507-516.
- Ross R. *The prevention of malaria*. London: John Murray, 1911.
- Rowe AK, Rowe SY, Snow RW, Korenromp EL, Schellenberg JRM, Stein C, Nahlen BL, Bryce J, Black RE, Steketee RW. The burden of malaria mortality among African children in the year 2000. *Int J Epidemiol* 2006; 35:691-704.
- Slooff R, Verdrager J. *Anopheles balabacensis* Baisas 1936 and malaria transmission in southeastern areas of Asia. 1972; WHO/MAL/72:765.
- Smalley ME, Sinden RE. *Plasmodium falciparum* gametocytes: Their longevity and infectivity. *Parasitol* 1977; 74:1-8.
- Smith DL, Dushoff J, Snow RW, Hay SI. The entomological inoculation rate and *Plasmodium falciparum* infection in African children. *Nature* 2005; 438:492-495.
- Taye A, Hadis M, Adugna N, Tilahun D, Wirtz RA. Biting behavior and *Plasmodium infection* rates of *Anopheles arabiensis* from Sille, Ethiopia. *Acta Tropica* 2006; 97:50-54.
- Tumwiine J, Mugisha JYT, Luboobi LS. A mathematical model for the dynamics of malaria in a human host and mosquito vector with temporary immunity. *Appl Math Comput* 2007; 189(2):1953-1965.
- Van den Driessche P, Watmough J. Reproduction numbers and sub-threshold endemic equilibria for compartmental models of disease transmission. *Math Biosci* 2002; 180:29-48.
- World Health Organization. *World Malaria Report 2008*.
- World Health Organization. *World Malaria Report 2010*.
- Zahar AR. Review of the ecology of malaria vectors in the WHO Eastern 4 Mediterranean region. *Bull World Health Organ* 1974; 50:427-440.

## Appendix A. Data for Baseline parameter value

This appendix shows the tables of data and explanations for the baseline parameter values of the model (2.9) including references.

**Population data for humans.** For areas with low transmission levels, Table A.1 shows the life expectancy and birth rate estimates for the year 2011 for the countries with areas of low transmission. Using the demographic data from the country of Rwanda, we assume the birth rate of 37 births per year per 1000 people, so  $\lambda_H = (37/365.25)/1000 = 0.000101$

For areas with high transmission levels, Table A.2 shows the life expectancy and birth rate estimates for the year 2011 for the countries with areas of high transmission. Using the demographic data from the country of Sao Tome Principe and assume a birth rate of 38 births per year per 1000 people, so  $\lambda_H = (38/365.25)/1000 = 0.000104$

**Population data for mosquitoes.** For the per capita natural birth rate of mosquitoes denoted by  $\lambda_v$ , we use the results for *An. gambiae* mosquito birth rate calculated by Olayemi and Ande (2009). The result from the study of 120 partially engorged adult female mosquitoes lived for an average of about 23 (23.1±8.29) days. A minimum of 10 days is required for *An. gambiae* mosquitoes to take their first blood meal and get infective, then the female mosquito will survive for an additional 13 days under controlled conditions. The computed overall survival rate from eclosion to adult emergence was 84.14%. For the per capita natural death rate of mosquitoes, we use the value  $\mu_v=0.052/\text{day}$ . The value used is similar to the value reported by Macdonald (1957). For both low and high areas of malaria transmission, we use the same value for  $\mu_v$ . For the range of values on both  $\lambda_v$  and  $\mu_v$ , we considered the same range used by Chitnis et al. (2008).

**Data for the number of bites on humans per female mosquito per unit time.** Table A.3 show results for the different estimates for the average number of bites on humans per female mosquito per day. As observed in the study of Taye et al. (2006), the biting cycle of mosquitoes in the indoor and outdoor environment appeared to be similar, but most biting of *An. arabiensis* occurred after 22:00 h when people are presumed to be in bed. For *An. arabiensis* and *An. gambiae*, the night biting cycle are similar with peak occurring between 2:00 and 6:00 (Fontenille et al. 1997). For our simulation, since malaria prevalence is shown to be higher on the children population (Gemperli et al. 2007, Bekessy et al. 1976), we assume a 15% increase on the number of bites on H1 compared to H2. For high transmission areas, we use the estimates of 0.40 bites per mosquito per day for  $a_2$  and 0.46 for  $a_1$ . For areas of low transmission, we use the estimated value of 0.25 bites per mosquito per day for  $a_2$  and 0.29 for  $a_1$ .

**Data for  $b$  and  $c$ .** Table A.4 shows the estimates from field studies, the probability of transmission from an infectious mosquito to a susceptible human. We use the estimate of  $b = 0.086$  for both low and high transmission countries. Table A.5 shows the probability of transmission from an infectious human to susceptible mosquitoes. We use the estimates of  $c = 0.48$  for areas with high level of transmission and  $c = 0.24$  for areas with low levels of transmission.

**Data for  $r_1$  and  $r_2$ .** Table A.6 shows estimates from field studies, the duration of the infectious period in humans. It has been shown that temporary immunity is slowly acquired and reduces illness when a person had repeated reinfection or continued exposure (Smith et al. 2005). Immunity to infection in early childhood do not persist, hence H1 will require a longer period to acquire some kind of immunity. To illustrate the behavior, we use 24 months for H1 to acquire temporary immunity and 9.5 months for the H2 class to clear infection and acquire some kind of immunity. We use selected values for both low and high transmission areas.

**Data for  $\nu_1$  and  $\nu_2$ .** Using the estimates in Table A.6, for the progression from the infectious state  $I_{h1}$  to susceptible state  $S_{h1}$ , we assume that it takes around 4 months, and for the progression from the infectious state  $I_{h2}$  to susceptible state  $S_{h2}$  to be around 2 years. We use the selected values for both low and high transmission areas.

**Data for  $\gamma$  and  $\gamma_2$ .** It has been shown that immunity in humans is short-lived and requires repeated reinfection to sustain itself. The rate at which the humans lose immunity is a nonlinear process that depends on the transmission rate (Smith et al. 2005). For ease of analysis, we assume that the immunity is lost at a constant rate. For our baseline value, we assume that the period of immunity for both H1 and H2 lasts for a year. This assumption will be used for both areas of low and high transmissions. We assume that the values vary from 3 months to 2 years.

**Data for  $\delta_1$  and  $\delta_2$ .** Table A.7 show estimates of the human population for areas of low and high level of malaria transmission. The computation for the per capita death rates of

humans due to infection, we use the reported death due to malaria from the World Malaria Report (WHO 2010). This will be done for the H1 and H2 population. For areas of low transmission, we use the estimate value of  $280/1694/1000/365.25 = 4.5 \times 10^{-7}$  for H1 and the estimate value  $529/8304/1000/365.25 = 1.7 \times 10^{-7}$  of for H2. Similarly, for areas of high transmission, we use the estimated values of  $2.1 \times 10^{-6}$  and  $9.8 \times 10^{-8}$  for H1 and H2 respectively.

**Data for  $\mu_1$  and  $\mu_2$ .** Table A.7 show estimates of the human population for areas of low and high level of malaria transmission. We use the values of death due to other causes in the computation for the per capita death rates of humans. This will be done for H1 and H2 populations.

**Data for  $\epsilon$ .** We use the range of values from the computed birth rate, the natural death rate (the other causes of death), and the death rate due to infection to estimate the value for  $\epsilon$ . We use an estimate of  $\epsilon$  by subtracting both the death rate due to infection  $\delta_i$  and the natural death rate  $\mu_i$  from the birth rate  $\lambda_i$ . The same formula will be used for both areas with low and high transmission. **PSL**

**Table A.1.** Demographic data for countries with areas of low level of malaria transmission.

Country	Life Expectancy (years)	Birth rate (total births per 1000 pop.)	Remarks
Madagascar	63.63	37.51	(CIA 2011)
Rwanda	58.02	36.74	(CIA 2011)
Swaziland	48.66	26.63	(CIA 2011)

**Table A.2.** Demographic data for countries with areas of high level of malaria transmission.

Country	Life Expectancy (years)	Birth rate (total births per 1000 pop.)	Remarks
Ethiopia	56.19	42.99	(CIA 2011)
Sao Tome Principe	63.11	38.03	(CIA 2011)
Senegal	59.78	36.73	(CIA 2011)
Zambia	52.36	44.08	(CIA 2011)

**Table A.3.** Daily mosquito biting rate

Human bites per mosquito	Mosquito	Year(s)	Location	Remarks
0.25	<i>An. balabacensis</i>	1964	Khmer	(Slooff and Verdrager 1972)
0.40	<i>An. punctulatus</i>	1957-1958	Maprik, New Guinea	(Peters and Standfast 1960)
0.25	<i>An. gambiae</i>	1967	Kankiya, Nigeria	(Garret-Jones and Shidrawi 1969)
0.47	<i>An. minimus</i>	1966-1967	Bangladesh	(Khan and Talibi 1972)
0.13	<i>An. gambiae</i>	1967	Khashm El Girba, Sudan	(Zahar 1974)
0.44	<i>An. gambiae</i>	1972	Garka, Nigeria	(Molineaux et al. 1979)

**Table A.4.** Probability of transmission of malaria from infectious mosquito to a susceptible human.

Probability of transmission	Comments	Remarks
0.0223 ± 0.0028	Calculations from data	(Nedelman 1985)
0.01	-	(Davidson and Draper 1953)
0.015-0.026	-	(Pull and Grab 1974)
0.06-0.27	Children	(Krafsur and Armstrong 1978)
0.05-0.13	Adults	(Krafsur and Armstrong 1978)
0.012	Village with highest mosquito density	(Nedelman 1984)
0.086	Village with lowest mosquito density	(Nedelman 1984)

**Table A.5.** Data for probability of transmission of infection from humans to mosquitoes.

Probability of transmission	Plasmodium	Time in days of gametocytemia	Remarks
0.24	<i>P. falciparum</i>		(Murhead-Thomson 1957)
0.48	<i>P. falciparum</i>		(Boyd 1941)
0.51	<i>P. falciparum</i>		(Draper 1953)
0.47	<i>P. falciparum</i>		(Draper 1953)
0.09	<i>P. falciparum</i>		(Draper 1953)
0.64	<i>P. falciparum</i>	1-4	(Smalley and Sinden 1977)
0.072	<i>P. falciparum</i>	11-12	(Smalley and Sinden 1977)
0.48			(Nedelman 1984)

**Table A.6.** Data for the duration of the infectious period for humans.

Infectious period (months)	Plasmodium	Comments	Remarks
2	<i>P. ovale</i>		(Molineaux and Gramiccia 1980)
4	<i>P. malariae</i>		(Molineaux and Gramiccia 1980)
9.5	<i>P. falciparum</i>		(Molineaux and Gramiccia 1980)
12-24	<i>P. falciparum</i>	No treatment	(Bloland et al. 2002)
18-60	<i>P. vivax</i>	No treatment	(Bloland et al. 2002)
18-60	<i>P. ovale</i>	No treatment	(Bloland et al. 2002)
36-600	<i>P. malariae</i>	No treatment	(Bloland et al. 2002)

**Table A.7.** 2009 data for countries with areas of low and high level malaria transmission.

Country	Death due to malaria		Other cause of death		Population (in 1000)		Remarks
	H1	H2	H1	H2	H1	H2	
Low Level							
Madagascar	80	93	519	2235	31047	16521	(WHO 2010)
Rwanda	280	529	1230	2980	1694	8304	(WHO 2010)
Swaziland	2	11	990	4375	160	1025	(WHO 2010)
High Level							
Ethiopia	212	909	1798	8483	13581	69244	(WHO 2010)
Sao Tome	18	5	275	630	23	140	(WHO 2010)
Senegal	216	358	3009	10024	2094	10440	(WHO 2010)
Zambia	1924	1938	15857	14282	2327	10608	(WHO 2010)